THE JOURNAL OF THE ACOUSTICAL SOCIETY OF KOREA VOL.25, NO.1E 2006, 3 pp. 1~7

Wave Reflection from Porous Ocean Sediment With Depth Dependent Properties

Keunhwa Lee*, Woojae Seong*
*Dept. of Naval Architecture and Ocean Engineering, Seoul National University, Seoul, KOREA
(Received November 8 2005; revised February 15 2006; accepted March 6 2006)

Abstract

This study examines the reflection characteristic of a thin transition layer of the ocean bottom showing variability with respect to depth. In order to model the surficial sediment simply, we reduce the Biot model to the depth dependent wave equation for the pseudo fluid using the fluid approximation (weak frame approximation). From the reduced equation, the difference between the inherent frequency dependency of the reflection and the frequency dependency resulting from a thin transition layer is investigated. Using Tang's depth porosity profile model of the surficial sediment [D. Tang et al., IEEE J. Oceanic Eng., vol.27(3), 546-560(2002)], we numerically simulated the reflection loss and investigated the contribution from both frequency dependencies. In addition, the effects of different sediment type and varying depth structure of the sediment are discussed.

Keywords: *Biot Model, Fluid Approximation of the Biot Model, Reflection Coefficient, Inherent Frequency Dependency, Global Matrix Method.*

I. Introduction

It is known that the wave in the ocean sediment is dispersive, which means that the sound speed and attenuation are dependent on frequency, and the reflection coefficient at an interface between water and sediment becomes frequency dependent[1].

If the geophysical properties of the ocean sediment vary significantly with depth, the reflection coefficient will exhibit an additional frequency dependency[2] besides the inherent frequency dependency due to dispersion. This dependency, due to interaction of the reflected waves within the depth dependent sediment, is governed by geometric factors such as the thickness of the transition layer and slope of variability. We will call it the geometric dispersion in this paper.

In recent fine-scale measurements of the surficial ocean sediment, a transition layer having thickness extending from a few mm to a few hundred mm has been found[3-4]. When the thickness of this transition layer is comparable to the wavelength, which corresponds to frequencies of at least several tens kHz, the transition layer will exhibit geometric dispersion. This means that distinction between the inherent and geometric frequency dependency of the reflection becomes obscure in mid-high frequency range. This obscurity can be a cause of error during the process of estimating the geophysical properties from reflection measurements.

A few authors have investigated the frequency dependency of the reflection from the ocean sediment. Chotiros[5] showed that the reflection measurement of sandy sediment significantly deviates from viscoelastic wave theory and confirmed the importance of the use of the geophysical model (Biot model) in ocean sediment.

Carbo[6] numerically showed that the transient layer reduces the amplitude of the reflected wave at high frequency, treating the ocean bottom as an acoustic medium approximated by the model suggested by Hovem for Biot's fast wave speed. Lyons and Orsi[3] confirmed the effect of the transition layer of varying density on the reflection. Masao[7] obtained the reflection

Corresponding author: Woojae Seong (wseong@snu.ac.kr)
Dept. of Ocean Engineering, Seoul National University, Shillim-dong Kwanak-ku Seoul 151-742, Korea

characteristic from the transition layer of the surficial sediment using OASES Biot the experimental result. All these studies separately have mentioned the inherent frequency dependency or the geometric frequency dependency of reflection from the ocean sediment. However, study on the effect of their combination has not been performed.

In this paper, we consider the reflection from the ocean sediment of varying geophysical properties. The ocean sediment is modeled by the fluid approximation of Biot model, which makes it an efficient numerical calculation model.

In order to describe the depth-dependent property of the sediment, we adopt the porosity profile presented by Tang et al. [4]. The numerical results are obtained using the direct global matrix approach[8].

In Sec. II, continuity equation and momentum equation for fluid approximation form of Biot model will be derived. In addition, the depth-dependent wave equation and the reflection coefficient will be obtained. The characteristic of the porosity profile and the choice of the Biot model parameters will be explained in Sec. III. Sec. IV will show the effect of the combination of both frequency dependencies. Sec. V is a conclusion.

II. FLUID APPROXIMATION OF BIOT MODEL AND THE REFLECTION COEFFICIENT

2.1. BIOT MODEL

Review of the Biot model employed will be given followed by simplification into an equivalent fluid model, which is used in the numerical analysis thereafter.

(a) Kinematics

If $\vec{u}_f$ is the fluid displacement vector, $\vec{u}$ is the solid displacement vector, and β is the porosity the strains are defined as [9],

$$e = \nabla \cdot \vec{u} \tag{1}$$

$$\varepsilon_{ij} = \frac{1}{2}(u_{i,j} + u_{j,i}) \tag{2}$$

$$\zeta = -\nabla \cdot (\beta(\vec{u}_f - \vec{u})) = -\nabla \cdot \vec{U}. \tag{3}$$

Here, e is the volumetric strain, ε_{ij} is the linear strain in the solid constituent, and ζ is the fluid increment.

(b) Stress-strain relation

The stress-strain relations for the total stress in the porous medium and the pore fluid pressure are

$$\tau_{ij} = ((H - 2\mu)e - C\zeta)\delta_{ij} + 2\mu\varepsilon_{ij} \tag{4}$$

$$p_f = M\zeta - Ce \tag{5}$$

where δ_{ij} is the kronecker delta.

Moduli M, C, and H are respectively,

$$M = K_r / [1 - K_b / K_r + \beta(K_r / K_f - 1)] \tag{6}$$

$$C = (1 - K_b / K_r)M \tag{7}$$

$$H = (1 - K_b / K_r)C + K_b + (4/3)\mu \tag{8}$$

where K_r is the solid bulk modulus, K_f is the fluid bulk modulus, K_b is the frame bulk modulus, and μ is the shear modulus.

(c) Momentum equation

The momentum equations are expressed as

$$\frac{\partial \tau_{ij}}{\partial x_i} = \frac{\partial^2}{\partial t^2}(\rho \vec{u} + \rho_f \vec{U}) \tag{9}$$

$$-\frac{\partial p_f}{\partial x_i} = \frac{\partial^2}{\partial t^2}(\rho_f \vec{u} + m\vec{U}) + \frac{\eta F(\kappa)}{k_s}\frac{\partial \vec{U}}{\partial t} \tag{10}$$

where ρ_f is the fluid density, ρ_s is the solid density and $\rho = (1-\beta)\rho_s + \rho_f\beta$ is the total density of the porous medium. Also, $m = \alpha\frac{\rho_f}{\beta}$ is the added mass density with the added mass parameter α, η is the fluid viscosity and k_s is the permeability.

The viscous correction factor $F(\kappa)$ can be expressed as

$$F(\kappa) = -\frac{1}{4}\frac{\sqrt{i\kappa}T(\kappa)}{1 - \frac{2T(\kappa)}{\sqrt{i\kappa}}} \tag{11}$$

where $T(\kappa) = \frac{J_1(\sqrt{i}\kappa)}{J_0(\sqrt{i}\kappa)}$ and $\kappa = a\sqrt{\frac{\omega\rho_f}{\eta}}$.

Here ω is the angular frequency and a is the pore size parameter. For convenience, we will use the following relation,

$$a \approx \frac{d}{3}\frac{\beta}{1-\beta} \tag{12}$$

where d is the grain size[10].

2.2. FLUID APPROXIMATION

(a) Continuity equation

If the frame bulk modulus K_b and shear modulus μ are assumed to vanish, then equations (4) and (5) become

$$\tau_{ij} = K\nabla\cdot(\vec{u}+\vec{U})\delta_{ij} \tag{13}$$

$$-p_f = K\nabla\cdot(\vec{u}+\vec{U}) \tag{14}$$

where $K = ((1-\beta)/K_r + \beta/K_f)^{-1}$.

The averaged displacement vector can be expressed as

$$(1-\beta)\vec{u}+\beta\vec{u}_f = \vec{u}+\vec{U} = \vec{u}_m . \tag{15}$$

Using the averaged displacement vector, equations (13) and (14) become as follows.

$$p = -K\nabla\cdot\vec{u}_m \tag{16}$$

where the pressure $p = p_f = -(1/3)\tau_{kk}$.

If we take the partial derivative with respect to time, equation (16) is seen to be the continuity equation of fluid medium that is rearranged by the equation of state and the linearization.

(b) Momentum equation

Under the same assumption of vanishing K_b and μ, equations (9) and (10) can be written as

$$\nabla(K\nabla\cdot(\vec{u}+\vec{U})) = \frac{\partial^2}{\partial t^2}(\rho\vec{u}+\rho_f\vec{U}) \tag{17}$$

$$\nabla(K\nabla\cdot(\vec{u}+\vec{U})) = \frac{\partial^2}{\partial t^2}(\rho_f\vec{u}+m\vec{U}) + \frac{\eta F(\kappa)}{k_s}\frac{\partial\vec{U}}{\partial t} \tag{18}$$

If we subtract equation (17) from equation (18) in the case of harmonic motion, the relation between the relative displacement and the solid displacement is obtained as follows.

$$\vec{U} = \frac{\rho_f-\rho}{\rho_f-m+\frac{j\eta F(\kappa)}{k_s\omega}}\vec{u} . \tag{19}$$

Substituting equation (19) into equation (17) and the reciprocal of equation (19) into equation (18), we obtain one equation as a function of $\vec{u}$ and one equation as a function of $\vec{U}$. Adding them and using the averaged displacement of equation (15), we obtain the following equation.

$$-\nabla p = \rho_{eff}(\omega)\frac{\partial^2\vec{u}_m}{\partial t^2} \tag{20}$$

where

$$\rho_{eff}(\omega) = \frac{\rho_f{}^2-\rho(m-\frac{j\eta F(\kappa)}{k_s\omega})}{2\rho_f-\rho-(m-\frac{j\eta F(\kappa)}{k_s\omega})} . \tag{21}$$

Equation (20) is the momentum equation for a porous medium with the assumption of the frame elastic modulus being zero. It is in the same form as the momentum equation of a fluid medium except for the complex density, which we will call as an effective density. We mention that the idea of this effective density was first proposed in Williams' work[11].

(c) Depth-dependent wave equation

We take the divergence of equation (20) and use equation (16) to obtain the governing equation in terms of pressure,

$$\rho_{eff}(\omega)\nabla\cdot(\frac{1}{\rho_{eff}(\omega)}\nabla p) = \frac{1}{c^2(\omega)}\frac{\partial^2 p}{\partial t^2} \tag{22}$$

where $c(\omega) = \sqrt{\frac{K}{\rho_{eff}(\omega)}}$. (23)

Equation (23) is the complex speed dependent on frequency. The accuracy of this approximation is confirmed in Ref 11. As frequency increases or the frame elastic modulus weakens, its accuracy gets better.

Meanwhile, if the displacements of the fluid and the solid move together, equation (23) becomes much simpler because the effective density becomes total density, which is known as Wood model.

2.3. THE REFLECTION COEFFICIENT

We consider the reflection of a plane wave from an interface

between homogenous water and sediment showing variability with respect to depth. In the water, the sound speed is denoted by c_1 and the density is denoted by ρ_1. Using the bottom impedance $Z(\omega)$, reflection coefficient can be written as

$$R(\omega)=\frac{Z(\omega)/\sin\theta_t - c_1\rho_1/\sin\theta_1}{Z(\omega)/\sin\theta_t + c_1\rho_1/\sin\theta_1} \tag{24}$$

where θ_1 is a grazing angle of the incident wave and $\sin\theta_t=\sqrt{1-(c(\omega)/c_1)^2\cos^2\theta_1}$. If the sediment is homogenous with respect to depth, the bottom impedance can be written using equation (20) for the interface condition as

$$Z(\omega)=c(\omega)\rho_{eff}(\omega) \tag{25}$$

The frequency dependency of equation (25) is the inherent property of the ocean sediment.

If the sediment has the variability with respect to depth, the bottom impedance can be expressed using equation (20) for the interface condition and equation (22) for the pressure in the sediment as follows[12].

$$Z(\omega)=\omega\rho_{eff}(\omega)\,p(\omega)\left(\frac{dp(\omega)}{dz}\right)^{-1}\Big|_{z=0} \tag{26}$$

where $z=0$ is the depth at the interface.

Equation (26) contains the effect of the inherent and geometric frequency dependency of the reflection.

III. DEPTH-DEPENDENT GEOPHYSICAL PROPERTIES

In Biot model, the microscopic structure of the sediment can be explained by its porosity, permeability, added mass parameter and pore size parameter.

In the case of depth-dependent sediment, these four properties will vary with depth. But the precise measurement of surficial sediment depth dependent properties is hard. Also, the measurement of all the microscopic properties has not been carried out until now.

Fortunately, the porosity has been measured with remarkable precision. Lyon and Orsi[3] presented the depth-porosity relation

Table 1. The parameters used in numerical simulation.

Parameter	Soft	Hard
Grain bulk modulus	3.6e+10 Pa	3.6e+10 Pa
Fluid bulk modulus	2.25e+9 Pa	2.25e+9 Pa
Grain density	2650 kg/m^3	2650 kg/m^3
Fluid density	1000 kg/m^3	1000 kg/m^3
Added mass parameter	0.25	0.25
Grain size	0.00038 cm	0.008 cm
Dynamic viscosity	0.001 $kg/m\cdot s$	0.001 $kg/m\cdot s$
Surficial porosity	0.9	0.7
Bottom porosity	0.76	0.47
Fitting parameter	ν =3.5	ν =3.5
	n =0.6	n =0.6

using the result measured by X-ray CT method. Tang et al.[4] also reported a useful relation using the conductivity measurement. The relation of Lyon and Orsi decays as $(1+az)^{-1}$ and that of Tang et al. decays as e^{-z^n}. The depth profile of Lyons and Orsi is smoother than that of Tang et al. for small depth and decays more slowly. In this paper, we choose the relation of Tang et al. The relation of Tang et al. is expressed as

$$\beta=\beta_0+(\beta_s-\beta_0)e^{-\nu z^n} \tag{27}$$

Where β_s is the porosity at $z=0$, β_0 is the porosity as $z\to\infty$, and ν and n are fitting parameters.

Fig. 1 shows the depth-porosity profile of Tang et al. The

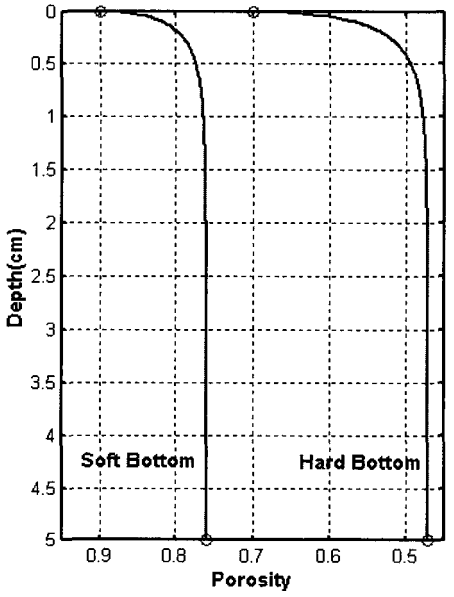

Fig. 1. The depth-porosity profile.

fitting parameter chosen by Tang et al. and the geophysical properties by Stoll are used. The values used in the calculation are given in Table I.

Aside from the porosity, other microscopic properties will be referred from previous empirical relations or treated as a constant value. The pore size parameter is obtained using equation (12) and the added mass parameter is considered as a constant value. The variability of the permeability is obtained with the Kozeny-Carman relation,

$$k_s = \frac{d^2}{36k_0}\frac{\beta^3}{(1-\beta)^2} \tag{28}$$

where k_0 is 5[6].

Other properties-i.e., density, bulk modulus and viscosity- are considered to be constant. Since the depth-dependency of the sediment is a response to bioturbation and hydrodynamic effects, these properties will have a low variability with respect to depth[3, 13].

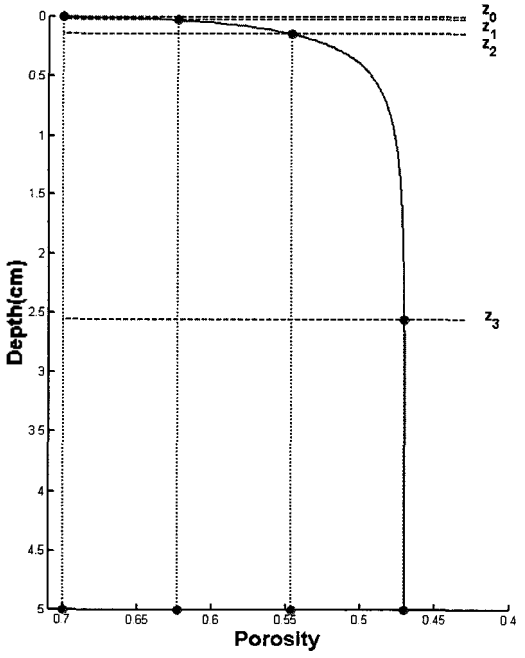

Fig. 2. The example of the division of sediment layer.

IV. NUMERICAL RESULT

In this section, we will present the numerical result using the data given in Table I. The porosity of the upper sediment is chosen a value satisfying the depth-porosity profile with a positive gradient.

As mentioned previously, the numerical result is obtained by using direct global matrix approach[8]. The DGM approach begins by dividing the inhomogeneous layer into several homogeneous layers. Here, we divide the transition layer uniformly based on porosity, not on depth, as shown in Fig. 2. This method has proven to produce faster convergence. To achieve a good approximation at high frequency, sediment layer is divided into 300 layers.

Fig. 3 shows the reflection coefficient as a function of grazing angle for frequencies of 10 kHz and 100 kHz for both soft and hard bottom. To investigate the effect of transition layer, the results are compared to no gradient case, meaning the sediment is considered as a homogeneous one. In Fig. 3, the effect of the depth-dependent property of the sediment is very small at 10 kHz, but at 100 kHz the sediment with gradient deviates from the sediment without gradient. Near normal incidence, the difference is about 2.7 dB for the soft bottom and the difference is about 2.2 dB for the hard bottom. This plainly shows the effect of a thin transition layer.

Since the effect of transition is most pronounced at normal incidence, we plot the normal reflection coefficient for varying frequency in Fig. 4. Solid curve represents homogeneous sediment, which only includes the effect of the inherent frequency dispersion. The difference of the normal reflection loss

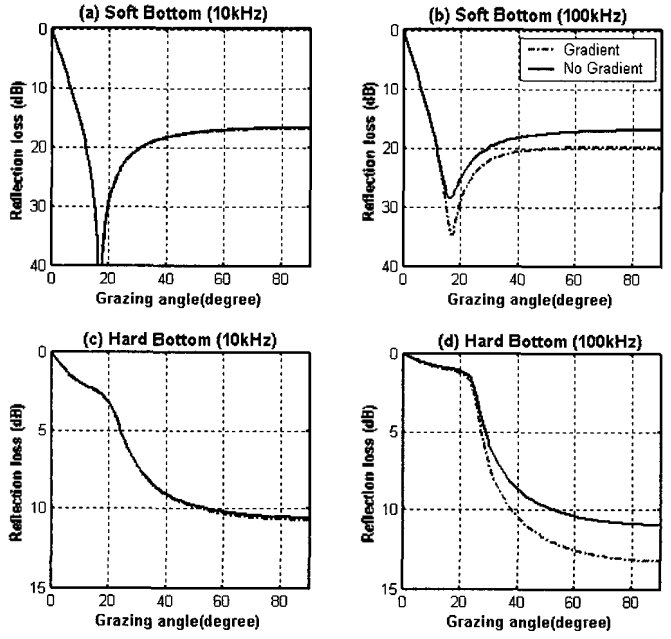

Fig. 3. The reflection loss versus the grazing angle at two frequencies for soft and hard bottom.

between 10^2 Hz and 10^6 Hz is about 1dB for both soft and hard bottom. The inherent frequency dispersion can be considered to be relatively weak. In addition, the hard bottom exhibits a set down at a relatively lower frequency because the critical frequency of the hard bottom is lower. The gradient case includes both the inherent and geometric frequency dispersion of the sediment. We can observe that the gradient case curve falls down more steeply than solid curve at high frequency for both bottoms. This is because the effect of the upper part of surficial sediment increases as frequency increases. Since its property is softer than that of the sediment at large depth, the reflection loss is seen to increase. If the surficial porosity is close to 1, the difference between the gradient and no gradient case becomes greater.

It is interesting that the deviation of solid and dash-dot curve happens at about 7 kHz, irrespective of the kind of bottom. This implies that the geometric frequency dispersion depends only on the depth structure of the sediment.

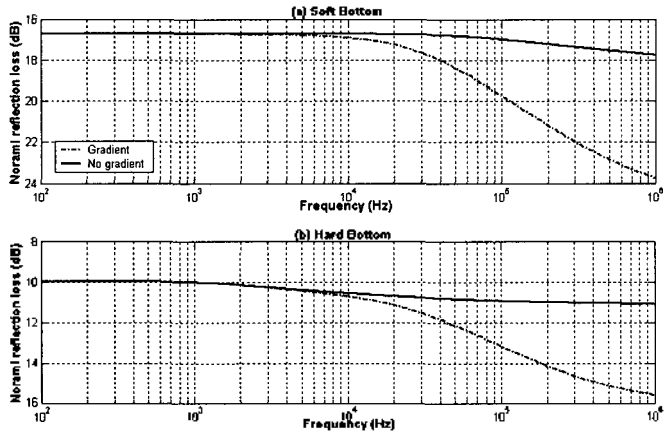

Fig. 4. The normal reflection loss versus frequency for soft and hard bottom.

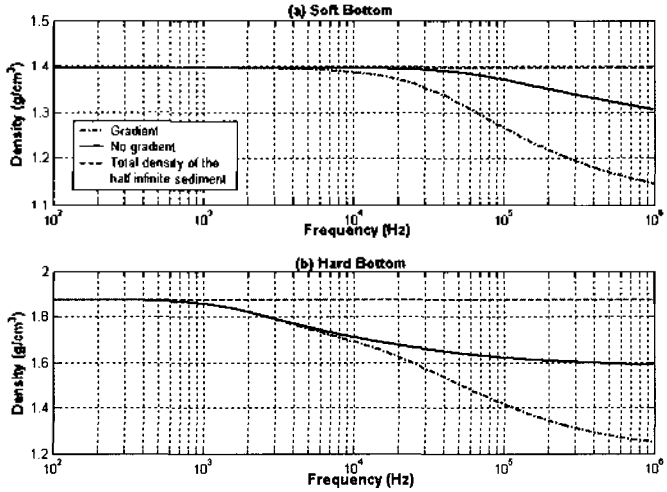

Fig. 5. The apparent density estimated from the normal reflection loss versus frequency for soft and hard bottom.

Fig. 5 shows the bottom density estimated from the normal reflection coefficient of Fig. 4. In fact, the quantity equivalent to the density, which is inverted from the reflection coefficient of equation (24) at normal incidence, isn't the real density. It is in the form of a complex density and quite different from the total density of the sediment.

But, if we assume the phase of the bottom impedance is negligible, we can obtain a quantity equivalent to the density.

With this assumption,

$$Z(\omega) = abs(Z(\omega))e^{j\phi(\omega)} \approx abs(Z(\omega)) \tag{29}$$

where $\phi(\omega) = \tan^{-1}(\mathrm{Im}(Z(\omega))/\mathrm{Re}(Z(\omega)))$.

The apparent density,

$$\rho_{app}(\omega) = abs(\frac{abs(Z(\omega))}{c_{ref}}) = \frac{c_1\rho_1}{abs(c_{ref})}(\frac{1+abs(R(\omega))}{1-abs(R(\omega))}) \tag{30}$$

can be derived from equation (24) and (29).

Here, c_{ref} is the reference speed, which is used to separate the quantity having the dimension of the density. We chose the reference speed as the sound speed of the half infinite sediment.

In Fig. 5, dash curve is the result obtained by modeling the bottom as an acoustic medium with half infinite sound speed and total density. At low frequency, all the apparent densities (solid and dash-dot curve) are close to dash curve. This is because the inherent and geometrical frequency dependency is negligible at low frequency. At high frequency, the apparent densities are lowered as the reflection loss increases. This result is to be expected from Fig. 4.

V. Conclusion

The reflection from surficial sediment having a transition layer is examined using a numerical model. Surficial sediment is considered to have the variability with respect to depth and is modeled by the fluid approximation of Biot model. We derived continuity equation, momentum equation, and depth-dependent wave equation for the surficial sediment. In order to investigate the depth-dependent property of the sediment, the depth-porosity profile of Tang et al. is used. Numerical simulation is performed using Direct Global Matrix method.

Considering the effect of the thin layer varying with respect to depth, we show that the normal reflection loss from sediment

increases at high frequency. The normal reflection loss with a homogeneous bottom is 11 dB at 100 kHz, but the normal reflection loss with the thin varying layer is 15.6dB at the same frequency for the hard bottom. It means that the thin varying layer at high frequency makes the sediment soft. The effect of the inherent frequency dependency is to raise the normal reflection loss at high frequency. Although its effect is smaller, it can affect the geophysical property estimated from the normal reflection loss.

References

1. R. D. Stoll, *Sediment acoustics, Springer-Verlag*, (NY, 1989)
2. L. M. Brekhovskikh, *Waves in layered media, Academic*, (NY, 1980)
3. A. P. Lyons and T. H. Orsi, "The effect of a layer of varying density on high-frequency reflection, forward loss, and backscatter," IEEE J. Oceanic Eng., **23** (4), 411-422, 1998.
4. D. Tang, K. B. Briggs, K. L. Williams, D. R. Jackson, E. I. Thorsos, and D. B. Percival, "Fine-scale volume heterogeneity measurements in sand," IEEE J. Oceanic Eng., **27** (3), 546-560, 2002.
5. N. P. Chotiros, "Inversion and sandy ocean sediment," in Full Field Inversion Methods in Ocean and Seismo Acoustics, edited by O.Diachok, A. Caiti, P. Gerstoft, and H. Schmidt (Kluwer, Dordrecht, 1995), 353-358.
6. R. Carbo, "Wave reflection from a transitional layer between the seawater and the bottom," J. Acoust. Soc. Am., **101** (1), 227
7. Masao Kimura and Takuya Tsurumi, "Characteristics of acoustic wave reflection from the transition layer of surficial marine sediment," in Proc. Underwater Technology 2002, 225-230.
8. F. B. Jensen, W. A. Kuperman, M. B. Porter, and H. Schmidt, *Computational ocean acoustics*, (AIP, NY, 1993)
9. M. Stern, A. Bedford, and H. B. Millwater, "Wave reflection from a sediment layer with depth-dependent properties," J. Acoust. Soc. Am., **77** (5), 1781-1788, 1985.
10. J. M. Hovem and G. D. Ingram, "Viscous attenuation of sound in saturated sand," J. Acoust. Soc. Am., **66** (6), 1807-1812, 1979.
11. K. L. Williams, "An effective density fluid model for acoustic propagation in sediments derived from Biot theory," J. Acoust. Soc. Am., **110** (5), pt1, 2276-2281, 2001.
12. S. R. Rutherford and K. E. Hawker, "Effects of density gradients on bottom reflection loss for a class of marine sediments," J. Acoust. Soc. Am., **63** (3), 750-757, 1978.
13. M. D. Richardson, D. K. Young, and K. B. Briggs, "Effects of hydrodynamic and biological processes on sediment geoacoustic properties in long island sound, U.S.A.," Marine Geology, **52**, 201-226, 1983.

[Profile]

•Keunhwa Lee

2000, Dept. of Naval Architecture and Ocean Eng., Seoul Nat'l Univ. (M.S)
2006, Dept. of Naval Architecture and Ocean Eng., Seoul Nat'l Univ. (Ph. D)
2006~Present, SNU Post-doctoral Associate.
※ Areas of interest: Ocean/sediment interaction problem, Target and diffuse scattering modeling, Inverse problem for the acoustic measurement.

•Woojae Seong

1982, Dept. of Naval Architecture, Seoul Nat'l Univ. (B.S)
1990, Dept. of Ocean Engineering, M.I.T. (Ph. D)
1991, MIT Post-doctoral Associate
1992~1996, Professor, Dept. of Ships and Ocean Eng., Inha Univ.
1996~Present, Professor, Dept. of Ocean Eng., Seoul Nat'l Univ.
※ Areas of interest: Propagation modeling, Geo-acoustic inversion, Matched field processing, Acoustic monitoring, Sonar applications for AUV.